Inhibition of tryptophan-dioxygenase activity increases the anti-tumor efficacy of immune checkpoint inhibitors

Florence Schramme[1,2], Stefano Crosignani[3], Kim Frederix[3], Delia Hoffmann[1,2], Luc Pilotte[1,2], Vincent Stroobant[1,2], Julie Preillon[3], Gregory Driessens[3], Benoit J. Van den Eynde[1,2,4;*]

[1] Ludwig Institute for Cancer Research, Brussels B-1200, Belgium.
[2] de Duve Institute, UCLouvain, Brussels B-1200, Belgium.
[3] iTeos Therapeutics, Rue des Frères Wright 29, 6041 Gosselies, Belgium.
[4] Walloon Excellence in Life Sciences and Biotechnology, Brussels B-1200, Belgium.
* Correspondence and Lead Contact: Benoît Van den Eynde
Mailing address: Avenue Hippocrate, 75 B1.74.03 – B-1200 Brussels, BELGIUM
Phone number: 0032 2 764 75 72
Email address: benoit.vandeneynde@bru.licr.org

Running Title: Anti-tumor synergy between TDO and checkpoint inhibitors

Keywords: Tumor resistance to immune response; Immunomodulation; Tryptophan 2,3-dioxygenase; TDO inhibitor; TDO knockout mice

Financial support for authors:

F. Schramme: Université catholique de Louvain
S. Crosignani: iTeos Therapeutics
K. Frederix; iTeos Therapeutics
D. Hoffmann: FNRS-FRIA (Grant number: 1.E082.14)
L. Pilotte: Ludwig Institute for Cancer Research
V. Stroobant: Ludwig Institute for Cancer Research
J. Preillon: iTeos Therapeutics
G. Driessens: iTeos Therapeutics
B. J. Van den Eynde: Ludwig Institute for Cancer Research

Disclosure of Potential Conflits of Interest:

S.C., K.F., J.P. and G.D. are employed by iTeos Therapeutics. B.V.d.E. is co-founder of, has ownership interest in, and is SAB member of iTeos Therapeutics.

Abstract

Tryptophan 2,3-dioxygenase (TDO) is an enzyme that degrades tryptophan into kynurenine and thereby induces immunosuppression. Like indoleamine 2,3-dioxygenase (IDO1), TDO is considered as a relevant drug target to improve the efficacy of cancer immunotherapy. However, its role in various immunotherapy settings has not been fully characterized. Here we describe a new small molecule inhibitor of TDO that can modulate kynurenine and tryptophan in plasma, liver and tumor tissue upon oral administration. We show that this compound increases the ability of checkpoint inhibitor anti-CTLA4 to induce rejection of CT26 tumors expressing TDO. To better characterize TDO as a therapeutic target, we also used TDO-KO mice and found that checkpoint inhibitors anti-CTLA4 or anti-PD1 induced rejection of MC38 tumors in TDO-KO but not in wild-type mice. Because MC38 tumors did not express TDO, we related this to the high systemic tryptophan levels in TDO-KO mice, which lack hepatic TDO needed to contain blood tryptophan. The effect of anti-PD1 was abolished in TDO-KO mice fed with a tryptophan-low diet that normalized their blood tryptophan level. Treatment of mice with an IDO1 inhibitor improved the efficacy of anti-PD1 in wild-type but not in TDO-KO mice. MC38 tumors express IDO1, whose activity limits the efficacy of anti-PD1 in wild-type mice but appears to be overcome in TDO-KO mice due to the high levels of tryptophan. These results support the clinical development of TDO inhibitors to increase the efficacy of immunotherapy, and suggest their use even in the absence of TDO expression at the tumor site.

Introduction

Cancer immunotherapy induces sustained clinical responses in a significant fraction of cancer patients (1,2). However, a majority of patients fail to respond. Several resistance mechanisms can be involved, including the presence of immunosuppressive pathways acting in the tumor microenvironment, some of which might be amenable to pharmacological inhibition, which could increase the efficacy of immunotherapy in combination (3,4). One of these mechanisms relies on the catabolism of L-tryptophan (Trp), which is converted into kynurenine (Kyn) by two distinct enzymes, indoleamine 2,3-dioxygenase (IDO1) and tryptophan 2,3-dioxygenase (TDO). Local tryptophan depletion combined with kynurenine production impairs cellular immunity, by reducing T-cell proliferation, inducing differentiation of regulatory T cells and driving dendritic cells towards a tolerogenic phenotype (5-7). In humans, IDO1 expression is restricted in normal tissues (8), but is strongly induced by interferon-gamma (IFNγ). Highly abundant in inflammatory sites, IDO1 appears to contribute to the winding down of the immune response to prevent immunopathology. In addition to this immunoregulatory effect, IDO1 activity can promote pathogenic inflammation favoring tumor angiogenesis (9). The exact mechanisms involved in the immunosuppressive effects of Trp catabolism by IDO1 remain unclear. In particular, the respective role of Trp depletion versus Kyn production in the microenvironment has been debated. Tryptophan depletion was initially suggested to impair T cell proliferation through the activation of an integrated stress response involving GCN2 stress kinase (10), but this was not confirmed in more recent studies ((11,12) and our unpublished results). Tryptophan depletion could also lead to deactivation of the mTOR pathway (13). Kynurenine and/or its derivatives, could also contribute to immunosuppression through the induction of T-cell apoptosis, the induction of regulatory T-cell differentiation, possibly via activation of the aryl hydrocarbon receptor (AhR), or the upregulation of PD-1 on $CD8^+$ T cells, also via AhR activation (14-18). Kyn degradation by *in vivo* administration of kynureninase was shown to increase the efficacy of checkpoint inhibitors or cancer vaccines (19). Altogether, IDO1 is largely described as an immunosuppressive protein, playing a major role in feto-

maternal tolerance (20), but also in cancer, as around 50% of human tumors express IDO1 (8,21). IDO1 expression in human tumors can either be constitutive, driven by cyclooxygenase-2 (22), or induced in response to IFNγ released by tumor-infiltrating lymphocytes in inflamed tumors such as melanomas (8,23,24). Tumoral expression of IDO1 is often associated with poor prognosis and a more aggressive tumor phenotype (8,25). IDO1 inhibitors (IDOi) have been developed and tested in numerous preclinical studies, showing synergistic anti-tumor activity when combined with immunotherapies such as vaccination or immune checkpoint blockade (21,26-28). These results have prompted the clinical development of IDOi which are tested for their ability to improve the clinical efficacy of immunotherapy (29,30). However, the first IDOi that completed Phase III testing proved disappointing, as it failed to improve the clinical activity of anti-PD1 in melanoma patients (31,32). The reasons for this clinical failure remain unclear at this stage, but could include, among others, an insufficient inhibition of IDOi activity and/or the involvement of other Trp-degrading enzymes (33,34).

The other enzyme that converts Trp into Kyn is TDO, which is encoded by gene *TDO2*. As opposed to IDO1, TDO is constitutively expressed at a high level in normal liver, where it degrades excess dietary Trp to maintain systemic levels around 80μM (23,35,36). This main function is illustrated by the 9-fold higher levels of Trp in the serum of the TDO-KO mice compared to wild-type (WT) mice (37). We previously reported the expression of TDO in human tumors, particularly in hepatocarcinomas, melanomas and bladder carcinomas (38). Although this study was performed by RT-PCR and the exact cell type(s) expressing TDO in these tumors remained to be defined, it suggested that TDO could contribute to tumoral immune resistance. A study published in 2011 also reported that human glioblastomas can express TDO and produce Kyn, which can activate AhR, enhance tumor cell survival and reduce infiltration by immune cells (39). We showed that TDO-transfected P815 mouse tumors resisted immune rejection by mice immunized against P1A, the dominant MAGE-type antigen expressed in these tumors (38). Importantly, tumor rejection was restored upon treatment of the mice with a TDO inhibitor (TDOi) (38). These results provided the proof of concept for the

clinical development of TDOi, which is ongoing. However, very few other studies have characterized the immunosuppressive role of TDO in cancers, which therefore remains much less known than that of IDO1. In particular, the immune effects of the modulation of systemic Trp by TDO inactivation have not been addressed. In this report, we further describe the role of TDO in modulating anti-tumor immune responses, using a novel TDOi as well as TDO-KO mice, and assessing the anti-tumor efficacy of checkpoint inhibitors. In a companion report, we characterize the expression of TDO in human tumors and normal tissues and define the TDO-expressing cell types and their impact on T-cell infiltration (40). These studies will help better define the place of TDOi in cancer immunotherapy.

Materials and methods

Cell lines

Mouse colon carcinoma lines MC38 and CT26 were obtained from Dr P. Berraondo (University of Navarra, Spain) and from ATCC respectively. CT26 cells were transfected with control vector (pCDneo, #15ACV2VC from GeneArt) or with a vector coding for mTDO (#15ADFX6C from GeneArt) using Lipofectamine 3000. CT26ev and CT26mTDO cells were selected with neomycin. Expression of TDO2 in CT26mTDO cells was validated by RT-PCR, WB and enzymatic activity assay (Supplementary Fig. S1). CT26mTDO cells were cultured in the presence of TDO inhibitor LM10 (20μM) (38,41).

Cellular assay for TDO inhibition

To determine the IC_{50} of PF06845102/EOS200809 on TDO-expressing cells, we used human glioblastoma cells A172, which constitutively express TDO (38,39); hTDO-transfected human cells 293-E hTDO (clone 119) (38); mTDO-transfected murine cells P815B-mTDO (clone 12) (38); murine cells CT26mTDO described above; hIDO1-transfected human cells 293-E hIDO1 (clone 17) and mIDO1 transfected murine cells P815B-mIDO1 (clone 6) (21,38). We transfected murine cells P815B with human TDO using the pEF6/V5His vector described in (38) to obtain P815B hTDO clone 19. We also transfected human 293-E and murine P815B cells with expression vectors pEF6/V5-His encoding the human IDO2 full-length (FL) or short-length (SL) open reading frame (starting at methionine 14, reportedly more active than the full-length (42) (ref seq: NM_194294)), to obtain 293-E hIDO2(FL) clone 5, P815B hIDO2(FL), P815B hIDO2(SL). The hIDO2(FL) was obtained from LPS-treated dendritic cells RNA using following primers: Fwd-AGG-CCA-CCA-CAA-GAA-TGT-TGC and Rev-GCA-GCC-TCC-TAA-CCA-CGT-G. The hIDO2(SL) ORF was subcloned from pEF6 hIDO2(FL) using following primers: Fwd-CTT-CAA-ACA-AAA-TAA-TGG-AGC-CCC-AC and Rev-GCA-GCC-TCC-TAA-CCA-CGT-G and inserted in vector pEF6/V5-His. The 2 plasmids were sequenced and we

excluded the presence of SNP rs10109853 (R248W polymorphism) (43). Expression of hIDO2(FL) and (SL) in both cell lines was validated by RT-PCR (Supplementary Fig. S2).

Cells were incubated ($2x10^5$ cells/well) in a final volume of 200µl of IMDM (80µM Trp) supplemented with 2%FCS in presence of the TDO inhibitor at different concentrations (1 – 10,000nM) for 24h. Cells were centrifuged and 55µl of supernatant were mixed with 55µl of 12% (wt/vol) trichloroacetic acid. After centrifugation, supernatants were used to quantify kynurenine concentration by HPLC-UV.

Mice

C57BL/6J Ola Hsd mice (Envigo), C57BL/6 IDO1-KO mice (Jackson Laboratory) and C57BL/6 TDO-KO mice (provided by Dr Hiroshi Funakoshi and Dr Toshikazu Nakamura from Osaka University) (37) were bred at the animal facility of the Ludwig Institute for Cancer Research, Brussels, Belgium. C57BL/6 and C57BL/6 TDO-KO mice were mated to obtain heterozygous offspring, which were intercrossed to obtain *Tdo*$^{+/-}$, *Tdo*$^{+/+}$ (WT) and *TDO*$^{-/-}$ (TDO-KO). Homozygous TDO-KO and WT mice littermates were selected by PCR on genomic DNA using primers: mTDO: Fwd-GTA-TCT-ATG-GAG-GAC-AAT-GAA-G, Rev-GAT-GAA-TAG-GTG-CTC-GTC-ATG; Neomycin: Fwd-GTT-CTT-TTT-GTC-AAG-ACC-GA, Rev-TTT-CCA-CCA-TGA-TAT-TCG-GC (Supplementary Fig. S3A). TDO-KO and IDO1-KO mice were mated to obtain double IDO1/TDO-KO mice, which were selected with the above TDO primers, and the following primers: IDO1: Fwd-TGG-AGC-TGC-CCG-ACG-C, Rev-TAC-CTT-CCG-AGC-CCA-GAC-AC; Neomycin: Fwd-CTT-GGG-TGG-AGA-GGC-TAT-TC, Rev-AGG-TGA-GAT-GAC-AGG-AGA-TC (Supplementary Fig. S3C). Homozygous IDO1/TDO-KO mice were then bred independently. BALB/c mice (Charles River) were maintained at the animal facility of the Institute for Medical Immunology, Gosselies, Belgium. Animal studies were conducted in accordance with national and institutional guidelines for animal care and with the approval of the *Comité d'Ethique pour l'Expérimentation Animale* from the *Secteur des Sciences de la Santé, UCLouvain* (2015/UCL/MD/14 and 2012-03 (BALB/c)).

183

184 ***In vivo* experiments**

185 Blocking monoclonal anti-CTLA4 (9H10), anti-PD1 (RMP1-14) and control isotype IgG2a (2A3)
186 were purchased from BioXCell. The standard and Trp-low diets were obtained from Special
187 Diet Services Ltd, based on Maeta *et al.* (44). Besides tryptophan, the two diets were similar
188 in composition, except for a small excess of the other essential amino acids in the Trp-low diet.
189 TDO inhibitor PF06845102/EOS200809 is described in published patent application
190 US 20150225367 (45). Epacadostat (Synnovator) (46) and TDO inhibitor
191 PF06845102/EOS200809 (both used at 100mg/kg, twice per day) were put in suspension after
192 10min sonication in methocel (vehicle). Tumors were measured twice a week and the volume
193 reported with the formula (l^2xL/2).

194

195 **Tryptophan and kynurenine quantification**

196 Sera were collected after 5min blood centrifugation (8000xg). Tumor interstitial fluids were
197 obtained by performing a low centrifugation (30min, 420xg, 10°C) on a 20µm nylon filter for
198 each total tumor sample as previously described (47). Tumor homogenates were harvested
199 after mixing pieces of 50 to 300mg tumor mass in PBS with Ultra-Turrax (IKA-T10, Sigma
200 Aldrich). Trp and Kyn concentration were quantified by LC-MS/MS or HPLC-UV analysis after
201 treatment with acetonitrile or trichloroacetic acid (TCA) (38).

202

203 **Quantitative RT-PCR**

204 Fifteen-micrometer thick frozen tumor sections were used for RNA extraction and RT-qPCR
205 with the following primers and probes (annealing 1min 60°C): βActin: Fwd-CTC-TGG-CTC-
206 CTA-GCA-CCA-TGA-AG, Rev-GCT-GGA-AGG-TGG-ACA-GTG-AG, Probe-ATC-GGT-GGC-
207 TCC-ATC-CTG-GC; IDO1: Fwd-GTA-CAT-CAC-CAT-GGC-GTA-TG, Rev-CGA-GGA-AGA-
208 AGC-CCT-TGT-C, Probe-CTG-CCC-CGC-AAT-ATT-GCT-GTT-CCC-TAC; TDO: Fwd-GTA-
209 TCT-ATG-GAG-GAC-AAT-GAA-G, Rev-GAT-GAA-TAG-GTG-CTC-GTC-ATG, Probe-CCT-
210 CCT-TTG-CTG-GCT-CTG-TTT-ACA-CC; CD8β: Fwd-GTG-GTT-GAT-GTC-CTT-CCT-ACA-

A, Rev-TCC-GCA-CAC-AGT-AAA-AGT-AGA-C, Probe-AAT-GCC-AGC-AGA-AGC-AGG-ATG-CAG-ACT-A; IFNγ: Fwd-TCA-AGT-GGC-ATA-GAT-GTG-GAA-GAA, Rev-TGG-CTC-TGC-AGG-ATT-TTC-ATG, Probe-TCA-CCA-TCC-TTT-TGC-CAG-TTC-CTC-CAG; Samples were assayed in duplicates and mRNA copies were calculated with internal standards and reported for 1000 cells (supposing a mean of 2000 βActin mRNA copies per cell).

Immunohistochemistry

MC38 tumors were frozen in Tissue-Tek O.C.T® Compound and seven-micrometer thick sections were obtained using a cryostat (CryoStar NX70, Thermo scientific). Thawed sections were fixed for 5min in 4% formaldehyde and antigen retrieval was performed by heating the sections in microwave 10mM citrate buffer pH6 0.05% Tween20. The detailed immunostaining protocol was previously described (22). The antibodies used were the following: rabbit anti-mouse CD8α mAb (clone D4W2Z, #98941T, Cell Signaling, dilution 1/1000), rabbit anti-human CD3 mAb (clone SP7, #16669, Abcam, dilution 1/200), rabbit anti-mouse CD4 mAb (clone EPR19514, #183685, Abcam, dilution 1/200) and labelled polymer-HRP goat anti-rabbit (Dako) as the secondary antibody. After washing, sections were finally stained with a 1/25 dilution of Highdef® DAB chromatogen (Enzo) in Highdef® DAB substrate buffer (Enzo) for 20min and counterstained with hematoxylin for 5min. Spleen was used as a positive control. Negative controls included liver and omission of primary antibody on duplicate tumor sections. Stained slides were mounted and digitalized with a Pannoramic P250 Flash III slide scanner (3DHISTECH) and were analyzed with CaseViewer (3DHISTECH). $CD8^+$, $CD4^+$ and $CD3^+$ cells were quantified with the Halo™ Image Analysis software. Invasive margins were defined by the software as 200µm-thick edges around tumor nests.

Statistical method

Statistical analyses were performed using Prism 6 (GraphPad Software). Comparison between two groups was performed using Mann-Whitney unpaired T-test, while two-way analysis of

variance (ANOVA) with Bonferroni post hoc test was used to compare the effects of different treatments on tumor growth. Survival curves were generated by Kaplan–Meier method and compared by using a log-rank test (Mantel–Cox).

The linear mixed model was obtained with the statistical software JMP, after log transformation of tumor volumes, where volumes smaller than $20mm^3$ where fixed at log(20). Fixed effects included time (third degree polynomial function), treatment and experiment with all their interactions. Random effects included a random intercept and slope per mouse. An average treatment difference in tumor growth over all experiments was tested by a joint hypothesis test for the interaction terms of time and treatment with effect coding of all categorical variables. Normalized tumor growth curves per experiment were constructed with the residual error term from a model as described previously without adding the treatment term. This way, only the variation caused by treatment remains, allowing to graphically assess a common treatment effect over all experiments.

Results

PF06845102/EOS200809 efficiently inhibits TDO activity *in vitro* and *in vivo*

We developed a new selective TDO inhibitor, starting from a high-throughput screening with recombinant hTDO, followed by hit-to-lead and lead-optimization medicinal chemistry steps (45). The final compound PF06845102/EOS200809, with structure shown in Table 1, was synthesized as described in (45) and found to inhibit the enzymatic activity of human TDO with an IC_{50} of 230nM and 285nM in a cellular assay using human glioma cells A172 (which constitutively express high levels of TDO) or hTDO-transfected 293-E cells, respectively (Table 1). It did not inhibit human IDO1 activity in transfected 293-E cells (Table 1). The inhibitor was also tested on cells expressing the full-length human IDO2 or the short, reportedly active form of hIDO2 (42), but these cells showed no tryptophan-degrading activity, indicating that hIDO2 is not active in physiological conditions, in line with the reported high K_m of the enzyme (6.8mM) (48). The compound also inhibited murine TDO activity (IC_{50} 104nM) while murine IDO1 activity was unaffected (Table 1). The pharmacokinetic properties of PF06845102/EOS200809 in mice were excellent (Table 1), with high exposures (AUC of 45000 h*ng/mL at 100mg/kg twice a day (BID)) and half-lives of 2.5h (IV) and 4h (PO), compatible with a good probability to achieve TDO inhibition *in vivo* with a BID administration. Exploratory toxicology studies performed in rats showed that the compound was well tolerated at doses of 30 and 100mg/kg and did not reveal any safety signals.

To confirm activity *in vivo*, we treated naive mice with increasing doses of TDO inhibitor by oral gavage. We collected liver and plasma and measured concentrations of kynurenine (Kyn) and tryptophan (Trp). We observed a dose-dependent decrease of Kyn in liver (Fig. 1A), and a concomitant increase of Trp in plasma (Fig. 1B), confirming a sustained *in vivo* inhibition of Trp degradation by TDO in the liver. Of note, kynurenine levels in the serum were not affected by TDO inhibition, in line with the notion that peripheral kynurenine, as opposed to hepatic kynurenine, is not produced by TDO but rather by IDO1 (see below). To confirm the activity of

the TDO inhibitor in the tumor-microenvironment, we established tumors by injecting mice with colon carcinoma CT26 cells transfected with an empty vector (CT26ev) or with a plasmid encoding mTDO (CT26mTDO). The latter cell line was confirmed to express TDO mRNA, protein and enzymatic activity (Supplementary Fig. S1A, B, C), while neither cell line expressed IDO1 or IDO2 (Supplementary Fig. S1A). In addition, TDO protein was detected by Western blot in explants from CT26mTDO but not from CT26ev tumors (Supplementary Fig. S1B). We treated mice with the TDOi (100mg/kg) by oral gavage and collected the tumoral interstitial fluid (ISF) 2h later. As expected, ISF from CT26mTDO tumors contained reduced Trp and increased Kyn levels as compared to control CT26 tumors (Fig. 1C). Upon treatment with PF06845102/EOS200809, Trp levels in ISF of CT26mTDO tumors were back to normal values indicating efficient inhibition of TDO (Fig. 1C). Of note, Kyn levels remained high in this setting, likely because of IDO1 expression induced in these tumors by the IFNγ produced by anti-tumor T cells (26) and because of increased availability of tryptophan as an IDO1 substrate. In the serum of CT26mTDO tumor-bearing mice treated with the inhibitor, tryptophan levels were increased while kynurenine levels were unaffected (Supplementary Fig. S4), similar to what happened in non-tumor-bearing mice (Fig. 1B).

Synergistic anti-tumor activity of TDO inhibition and checkpoint inhibition

To evaluate the anti-tumor effect of TDO inhibition in combination with the administration of checkpoint inhibitors, we used the CT26mTDO model described above. This was needed because we could not identify a mouse tumor line expressing TDO naturally (see below), in contrast with human tumor lines, several of which constitutively express TDO at a high level (38). We inoculated BALB/c mice subcutaneously with CT26mTDO cells or CT26ev cells. Nine days later, we injected mice with anti-CTLA4 antibody, and/or treated them with PF06845102/EOS200809 by oral gavage (Fig. 2). Monotherapy with anti-CTLA4 or TDO inhibitor did not significantly affect progression of either tumor type. However, in mice with CT26mTDO tumors that received the combination of anti-CTLA4 and TDO inhibitor, we observed an increased antitumor efficacy, with 6/10 mice showing complete regression and

no palpable tumor after 100 days, as compared to 2/10 mice treated with anti-CTLA4 single agent (Fig. 2A). The combined treatment was not effective in mice with control tumors CT26ev, which did not express TDO (Fig. 2B). In total, the effect of the combination was compared to anti-CTLA4 monotherapy in 3 independent experiments with CT26mTDO tumors. Although a high degree of individual variability was present in all experiments, we observed, in each experiment, more mice with regressing tumors in the combination group as compared to the monotherapy group. This difference became obvious when the tumor growth curves of all 3 experiments were combined and normalized to be plotted on the same scale (Fig. 2C). Overall, the anti-tumor effect of the combination group compared to anti-CTLA4 was highly significant ($p=0.0004$).

These results indicate a synergistic anti-tumoral effect of TDO inhibition and anti-CTLA4 therapy in TDO-expressing CT26 tumors. These data further document the immunosuppressive role of TDO in the tumor microenvironment, and indicate that TDO inhibitors could be used in combination with checkpoint inhibitors in patients bearing TDO-expressing tumors.

Lack of spontaneous TDO expression in mouse tumors

So far, available evidence supporting an immunosuppressive role of TDO in cancer was obtained with murine cell lines transfected with TDO2. Several human tumor cell lines do express TDO naturally, and a number of human tumor samples express TDO2 mRNA, indicating natural expression of TDO in the tumor microenvironment (23,38). To better mimic the human situation, we searched for murine tumors that express TDO naturally. We collected a series of primary tumors and metastases obtained by implanting common tumor lines into syngeneic mice or by injecting tamoxifen into genetically engineered TiRP melanoma mice (49,50) (Supplementary Table S1). We collected tumors at different time points and measured TDO2 expression by RT-qPCR. Surprisingly, none of these 15 tumor models expressed TDO2

transcripts. These data suggest that, unlike human cancers, mouse tumors do not contain TDO-expressing cells.

Increased efficacy of checkpoint inhibitors in TDO-KO mice

In parallel to these studies, we also injected a series of mouse tumor lines into TDO-KO mice, to investigate the potential role of host TDO expression. Because of the lack of hepatic TDO expression, these mice have a defect in tryptophan homeostasis and were reported to have higher levels of systemic tryptophan (37). In line with this, we measured an increased Trp concentration in the serum of the TDO-KO mice (430µM) as compared to their WT or heterozygous (70 to 100µM) counterpart (Fig. 3A and Supplementary Fig. S3B). The link between TDO deficiency and high tryptophanemia is supported by the observation of similar metabolic changes in an independent strain of TDO-KO mice (51) and in a human with inherited TDO deficiency, who presented chronic hypertryptophanemia (52). In contrast, IDO1-KO mice had normal Trp levels in their serum. Kynurenine, the main product of both TDO and IDO1, was increased in TDO-KO mice but was totally absent in IDO1-KO mice (Fig. 3B). This observation indicates that circulating kynurenine is produced by IDO1 but not by TDO. This is likely because the kynurenine produced by TDO is further degraded in the liver, which expresses all the enzymes of the kynurenine pathway, while the inflammatory and immune cells that express IDO1 in the periphery do not express these enzymes. The higher kynurenine levels observed in TDO-KO mice would result from higher amounts of tryptophan being degraded by IDO1 in peripheral tissues. This is entirely related to the increased levels of circulating tryptophan – the IDO1 substrate – in these mice, as we found no increased IDO1 or IDO2 expression in tissues (liver, colon and lymph nodes) from TDO-KO mice as compared to WT mice (Supplementary Fig. S5). In line with the role of IDO1 in producing systemic kynurenine, we measured almost no kynurenine in the serum of double KO mice ($IDO1^{-/-}$ $TDO^{-/-}$), despite very high tryptophan levels (Fig. 3A, B). These results indicate that TDO activity, by degrading dietary tryptophan, maintains tryptophan homeostasis by reducing blood levels of tryptophan, while blood kynurenine is produced exclusively by IDO1 in the periphery.

Even though in the meantime we observed no TDO expression in murine tumors, we were still interested to see whether the drastic changes in systemic tryptophan metabolism observed in TDO-KO mice would affect anti-tumor immune responses, given the high sensitivity of T-cell mediated responses to tryptophan catabolism (10,13,53-55). We used the colon adenocarcinoma line MC38, described as being immunogenic (56-58) and able to generate liver metastases (59-61). We counted the number of liver metastases (LM) three weeks after intrasplenic injection followed by hemisplenectomy in TDO-KO and WT littermate mice. Although 62% (26 out of 42) of WT mice developed metastases, only 36% (15 out of 42) of TDO-KO mice did. The average number of metastases was also slightly reduced in LM-bearing TDO-KO mice (11 LM/mouse) as compared to LM-bearing WT mice (18/mouse), but this difference was not significant (Supplementary Fig. S6). These results suggested that TDO-KO mice were more resistant to metastasis development, potentially because of a better anti-tumor immune response.

To further explore this point, we evaluated the primary growth of subcutaneous MC38 tumors. We observed similar growth rates in TDO-KO and WT littermate mice. However, upon treatment with immune checkpoint inhibitor anti-CTLA4 (Fig. 4A) or anti-PD1 (Fig. 4B), we observed a significant decrease of tumor growth in TDO-KO mice but not in WT littermates. To confirm the involvement of T cells in this difference, we collected tumors and analyzed the expression of CD8β by RT-qPCR, as a measure of CD8 T-cell infiltration. CD8β mRNA expression was significantly increased in tumors from TDO-KO mice treated with anti-PD1, while they were not in WT mice treated with anti-PD1 (Fig. 4C). We also evaluated T-cell infiltration by immunohistochemistry in MC38 tumors, and quantified the cells expressing CD8, CD4 or CD3 in the invasive margin and the central tumor region (Fig. 4D, E, F). We confirmed a higher $CD8^+$ cell infiltration in tumors from TDO-KO as compared to WT mice, while there was no clear difference for $CD4^+$ and $CD3^+$ cells. Of note, there was no difference in the proportion of $CD4^+$ and $CD8^+$ T cells in the spleen and PBMC of TDO-KO and WT naive non-

tumor bearing mice, as measured by flow cytometry. Altogether, these results suggest that immune checkpoint inhibitors induce stronger anti-tumor $CD8^+$ T cell response in TDO-KO mice as compared to WT mice, resulting in better tumor control.

Loss of efficacy of anti-PD1 upon of normalization of systemic tryptophan levels

To determine whether this better efficacy of checkpoint inhibitors was related to the high systemic Trp and Kyn concentrations, we tried to normalize blood Trp and Kyn levels by changing the diet of TDO-KO mice. After 24h of feeding on a diet with a Trp content reduced from 0.18% to 0.06%, the blood of TDO-KO mice contained normal levels of Trp and Kyn (Supplementary Fig. S7), while their weight and behavior were similar to those of mice fed with standard diet. We then repeated the anti-PD1 experiment with MC38 tumors in TDO-KO mice fed with either standard or low-Trp diet. Interestingly, while anti-PD1 showed again anti-tumor efficacy in TDO-KO mice fed with standard diet, this was no longer the case when TDO-KO mice were fed with Trp-low diet (Fig. 5A, B). At the end of the experiment, we collected serum and tumors and analyzed Trp and Kyn concentrations by HPLC. Again, the six-fold higher Trp levels observed in the serum of TDO-KO mice were reduced when the mice were fed on Trp-low diet, down to levels equal or below those of WT mice fed on standard diet (Fig. 5C). Levels of Trp in the tumor homogenate and interstitial fluid reflected those in the blood, with high levels (600µM) in TDO-KO mice fed on standard diet and lower levels in TDO-KO fed on Trp-low diet, which were similar to those of WT mice (Fig. 5D, E). Interestingly, the Kyn concentrations in the tumor homogenate and in the interstitial fluid from the TDO-KO mice were not or only barely affected by the diet change. These results indicate that the high systemic Trp concentration observed in TDO-KO mice is required for the anti-tumoral effect of the anti-PD1.

Role of IDO1 expression in tumors

To explain this observation, we considered that MC38 tumors might express IDO1 and thereby suppress proliferation and/or activity of anti-tumor T lymphocytes in WT mice by degrading Trp

421 locally. In TDO-KO mice, the very high Trp concentration at the tumor site might overload IDO1
422 activity and prevent it from reducing Trp down to the levels required for immunosuppression.
423 To test this hypothesis, we measured the expression of *IDO1*, *IFNγ* and *TDO2* by RT-qPCR in
424 the tumors from TDO-KO and WT mice treated with anti-PD1 or IgG2a, collected between 6
425 and 15 days after MC38 challenge (Fig. 6A). The results confirmed a significant expression of
426 *IDO1* in these tumors, which was slightly increased after anti-PD1 treatment. A similar pattern
427 was observed for IFNγ, indicating an ongoing immune response. As expected, no *TDO2*
428 expression was detected in any of the MC38 tumor samples. These tumors contained high
429 Kyn concentrations, which were increased 4 to 7-fold in both the tumor homogenate and the
430 tumor interstitial fluid as compared to the levels measured in the serum (Fig. 5C, D, E). Since
431 TDO is not expressed in these tumors, this high Kyn concentration can only be due to IDO1
432 activity.
433
434 To confirm the role of IDO1, we then inhibited IDO1 activity *in vivo* using epacadostat,
435 considering that if IDO1 was indeed responsible for the lack of effect of anti-PD1 in WT mice,
436 then its inhibition should increase anti-PD1 efficacy in WT mice, but not in TDO-KO mice
437 because IDO1 activity would already be functionally “inactivated” by the high Trp levels. We
438 administered epacadostat twice a day by gavage in TDO-KO or WT mice bearing MC38 tumors
439 and treated with anti-PD1. As shown in Fig. 6B and 6C, IDO1 inhibition strongly improved the
440 anti-tumor effect of the anti-PD1 in WT mice, but had no effect in TDO-KO mice. At the end of
441 the experiment, we collected the serum and the tumor homogenates to measure Trp and Kyn
442 (Supplementary Fig. S8). Epacadostat administration did not increase Trp levels, which
443 remained high in TDO-KO and low in WT mice. However, Kyn levels were reduced in samples
444 from mice receiving epacadostat, both in sera and tumor homogenates, in line with IDO1
445 inhibition.
446
447 Altogether, these results suggest that the increased systemic levels of tryptophan resulting
448 from TDO inactivation can overcome local immunosuppression induced by IDO1 expression

449 at the tumor site. Therefore, TDO inhibitors might be used in cancer patients to increase the
450 efficacy of immunotherapy, even if the absence of TDO expression at the tumor site.

Discussion

Our results confirm the benefit of blocking TDO activity to increase the efficacy of immunotherapy. This is based on experiments using the novel TDO inhibitor PF06845102/EOS200809, which was optimized for in vivo application and further clinical development. Like previously described inhibitors 680C91 and LM10, EOS200809 is based on a 6-fluoro indole scaffold (38,41,62). However, when tested side-by-side in a standardized cellular assay, it is two times more potent than 680C91, and more than 100-fold more potent than LM10 (Supplementary Table S2). It is also more selective, particularly with regard to several important heme-containing cytochromes, which are significantly inhibited by 680C91 but not by EOS200809 (Supplementary Table S2). Compound 680C91 also suffers from poor stability in human and mouse microsomes, and this parameter is also improved with EOS200809, whose microsomal intrinsic clearance is divided by three on both human and mouse microsomes (Supplementary Table S2). The good metabolic stability of EOS200809 was confirmed in mouse pharmacokinetic studies, which showed the compound as moderately cleared (30 mL/min/Kg) and with excellent oral bioavailability (80% at 100 mg/kg), giving exposures (AUC 45000 h*ng/mL at 100 mg/kg, $C_{average}$ 5200 nM) sufficient to achieve good TDO target coverage in vivo (Table 1). These features are drastically improved as compared to 680C91, which is known to be poorly bioavailable through the oral route (38). They are in line with our observation that ESO200809 can increase blood tryptophan levels more than twofold upon oral administration (Fig. 1). A recent comprehensive review compiled the structure and features of TDO inhibitors described in the patent literature, including EOS200809 (63). Although a few compounds show *in vitro* activity similar to EOS200809, no pharmacokinetic/pharmacodynamic data is available for these compounds. EOS200809 is therefore the first TDO-selective inhibitor reported with a favorable pharmacokinetic/pharmacodynamic profile after oral administration, allowing its preclinical evaluation *in vivo* in mouse tumor models and its potential subsequent clinical development.

Indeed, we report here a synergistic activity of EOS200809 when used in combination with checkpoint inhibitor anti-CTLA4 to treat tumors obtained with CT26 tumor cells engineered to express TDO (Fig. 2). It was not possible to test this approach with mouse tumors expressing naturally TDO, because no such tumors could be identified among the 15 mouse tumors that we screened. However, a number of human tumors were shown to naturally express TDO (38,39). Therefore, the results obtained with CT26-mTDO tumors are relevant to human TDO-expressing tumors, and confirm previous observations indicating immune escape of TDO-expressing tumors (39), including our findings that rejection of TDO-transfected P815 tumors by immune mice can be restored upon treatment with a TDO inhibitor (38). However, the current report is the first to describe the synergy between a checkpoint inhibitor and a TDO inhibitor. The expression of TDO in human tumors, which has now been extensively characterized using novel antibodies, is described in details in the accompanying report (40). Some tumors, such as hepatocarcinoma, constitutively express TDO at a high level in the tumor cells themselves and represent prime indications for TDO inhibitors (23). Other tumors, including glioblastomas, bladder, pancreatic and colon carcinomas, express TDO in stromal cells belonging to the tumor vasculature (40). The testing of TDO inhibitors in clinical trials is therefore warranted, particularly in view of the failure of the first clinical trial testing IDO1 inhibitor epacadostat in combination with anti-PD1 (31). Although there are many potential reasons for this outcome, it is not impossible that IDO1 inhibitors need to be combined with TDO inhibitors to reveal their full potential (33,34).

Recent work using IDO1-KO mice has revealed additional roles of IDO1-mediated tryptophan catabolism in shaping a protumorigenic type of inflammation that favors angiogenesis and recruitment of MDSC (9,64-66). IDO inhibitors were also reported to synergize with immunogenic chemotherapy in autochthonous mouse tumor models (64,67-71). Although TDO expression in non-hepatic tissues is limited, it will be interesting to determine whether TDO plays a similar inflammatory modulator role and whether TDO inhibitors could also synergize with chemotherapy.

Intriguingly, we observed that modulating TDO activity can also regulate immune responses against tumors that do not express TDO. This was based on a better efficacy of checkpoint inhibitors to induce rejection of MC38 tumors in TDO-KO mice as compared to wild-type mice (Fig. 4). Because these tumors do not express TDO, this effect depends on the increased circulating levels of tryptophan observed in TDO-KO mice, resulting from the missing function of liver TDO to degrade excess dietary tryptophan and regulate tryptophan homeostasis. Accordingly, the anti-tumor effect of anti-PD1 was lost when TDO-KO were fed a Trp-low diet that normalized circulating Trp levels (Fig. 5). We inferred that high Trp levels in the blood and tumors of TDO-KO mice can overcome the capacity of locally expressed IDO1 to induce a Trp depletion that is sufficient to induce effective immunosuppression. In line with this explanation, we found IDO1 to be expressed in these MC38 tumors (Fig. 6A), and we observed that treatment of WT mice with IDO1 inhibitor epacadostat restored a similar efficacy of anti-PD1 as that observed in TDO-KO mice (Fig. 6B, C). Altogether, these results suggest that TDO inhibitors might be clinically beneficial also for the treatment of human tumors expressing little or no TDO, provided that they can increase systemic Trp to levels similar to those present in TDO-KO mice. At least two published reports support this notion that inhibition of hepatic TDO may help anti-tumor immunity. The first is our previous study of TDO-expressing P815 tumors, in which we surprisingly observed that the TDO inhibitor LM10 also promoted better rejection of control P815B tumors that did not express TDO (38). Another recent paper showed a decrease in the number of lung metastases in mice inoculated intravenously with Lewis lung carcinoma (LLC) cells and subsequently treated with the TDO inhibitor 680C91 (72). This is also in line with the reduced number of liver metastases we observed in TDO-KO mice injected with MC38 tumors, although in this case hepatic TDO activity could also play a role locally in WT mice.

The respective role of IDO1 and TDO in tryptophan homeostasis has been unclear. The results reported here provide some clues in that respect, by describing, for the first time, mice that are

knockout for both IDO1 and TDO, which are viable and fertile. We confirm the previous reports describing high levels of both Trp and Kyn in the blood of TDO-KO mice (37). The high Trp levels are explained by the loss of liver TDO activity required to degrade excess dietary Trp. The higher Kyn levels were more difficult to explain, and presumably resulted from Trp degradation by IDO1, occurring in the periphery in the few IDO1-expressing cells, namely dendritic cells in lymphoid organs, inflammatory cells and some scattered cells in the lung, the female genital epithelia and, in the mouse, the epididymis (8). Kyn production by IDO1 is enhanced by increased levels of Trp, even though expression of IDO1 or IDO2 is not increased in TDO-KO mice. Our study fully confirms this prediction, by showing that both IDO1-KO and double IDO1/TDO-KO mice have barely detectable Kyn levels in their blood (Fig. 3). We conclude that the circulating level of Trp is controlled by hepatic TDO, while circulating Kyn is produced by IDO1 in the periphery.

Our results also shed some light on the respective role of Trp depletion and Kyn production in the immunosuppression triggered by Trp catabolism. We observed that the 7-fold higher Trp level present in the blood of TDO-KO mice was solely responsible for the increased anti-tumor effect of anti-PD1. In fact, these mice had normal to elevated Kyn levels. When TDO-KO mice were fed with a Trp-low diet able to normalize circulating Trp levels, the anti-tumor effect of anti-PD1 was lost. In this setting, Kyn circulating levels were also reduced (Fig. 5). Hence, the increased efficacy of anti-PD1 in TDO-KO mice and its loss upon dietary Trp restriction does not fit with a major immunosuppressive role of Kyn in this setting. On the other hand, a major role for Trp depletion would imply that, in WT mice, some extracellular regions of the tumor microenvironment exhibit a low Trp concentration and locally impact tumor-infiltrating T cells. This was not clearly observed in our measurements of Trp concentration in tumor homogenates or interstitial fluid, in which Trp concentration remained at a physiological level (~ 80 to 120µM) (Fig. 5). Two reasons may explain this result. Firstly, it is likely that intracellular Trp is much higher than extracellular Trp, particularly in tumors expressing IDO1 or TDO, which were shown to overexpress solute carrier transporters (SLC) involved in Trp uptake, such as

SLC7A5 and SLC1A5 (73-76). That is the reason we tried to analyze interstitial fluid in addition to tumor homogenates. Even though the protocol we used to collect interstitial fluid was conceived to limit contamination by intracellular fluid (47), we cannot exclude some cell lysis during the centrifugation step, resulting in overestimation of the actual Trp levels in the extracellular environment. To avoid this bias, it might be useful in future studies to use a better method to collect extracellular fluid, e. g. by microdialysis (77). Secondly, it is possible that extracellular Trp is reduced only in certain areas of the tumor, affecting T cells locally. In this context, a recent report showed that quantitative mass spectrometry imaging allowed to study the spatial distribution and quantitation of Kyn and Trp in IDO1-expressing tumors (78). Although Trp levels appear to play an important role, our results do not rule out an immunosuppressive role of Kyn. Trp levels in the blood and in the tumor homogenate were barely affected by treatment of both TDO-KO and WT mice with IDO1 inhibitor epacadostat, while Kyn levels were strongly reduced in both mouse strains (Supplementary Fig. S8). This is consistent with proper inhibition of IDO1 activity, which increases the efficacy of anti-PD1 in WT mice. As discussed above, our experimental approach did not capture real concentrations of extracellular metabolites in subareas of the tumor microenvironment. However, these results suggest that both high Trp (TDO-KO mice) and low Kyn (epacadostat) may contribute to relieving immunosuppression orchestrated by the IDO1/TDO pathway.

Acknowledgements

We thank Dr Hiroshi Funakoshi, Dr Toshikazu Nakamura and Dr Michaël Platten for providing TDO-KO mice; Christophe Lurquin, Pedro J Gomez Pinilla, Guy Warnier and the LAF team for the production and the genotyping of TDO-KO, IDO1-KO and IDO1/TDO-KO mice; Sofie Denies for statistical advice; and Auriane Sibille for editorial assistance.

Funding

This work was supported by Ludwig Cancer Research, the Fonds Scientifique pour la Recherche – FNRS, de Duve Institute and Université catholique de Louvain (Belgium).

Author Contributions

Conception and design : F.S., G.D. and B.V.d.E.

Methodology : F.S., G.D. and B.V.d.E.

Acquisition of data : F.S., K.F., D.H., L.P., V.S., J.P., H.F., T.N. and S.C.

Writing – Original Draft : F.S., G.D. and B.V.d.E.

Study supervision : G.D. and B.V.d.E.

References

1. Khalil DN, Smith EL, Brentjens RJ, Wolchok JD. The future of cancer treatment: immunomodulation, CARs and combination immunotherapy. *Nat Rev Clin Oncol* **2016**;13(5):273-90.
2. Tran E, Robbins PF, Rosenberg SA. 'Final common pathway' of human cancer immunotherapy: targeting random somatic mutations. *Nat Immunol* **2017**;18(3):255-62.
3. Liu Y, Cao X. Immunosuppressive cells in tumor immune escape and metastasis. *J Mol Med (Berl)* **2016**;94(5):509-22.
4. Rieth J, Subramanian S. Mechanisms of Intrinsic Tumor Resistance to Immunotherapy. *Int J Mol Sci* **2018**;19(5).
5. Munn DH, Mellor AL. Indoleamine 2,3 dioxygenase and metabolic control of immune responses. *Trends Immunol* **2013**;34(3):137-43.
6. Mellor AL, Baban B, Chandler P, Marshall B, Jhaver K, Hansen A*, et al.* Cutting edge: induced indoleamine 2,3 dioxygenase expression in dendritic cell subsets suppresses T cell clonal expansion. *J Immunol* **2003**;171(4):1652-5.
7. Pallotta MT, Orabona C, Volpi C, Vacca C, Belladonna ML, Bianchi R*, et al.* Indoleamine 2,3-dioxygenase is a signaling protein in long-term tolerance by dendritic cells. *Nat Immunol* **2011**;12(9):870-8.
8. Theate I, van Baren N, Pilotte L, Moulin P, Larrieu P, Renauld JC*, et al.* Extensive profiling of the expression of the indoleamine 2,3-dioxygenase 1 protein in normal and tumoral human tissues. *Cancer Immunol Res* **2015**;3(2):161-72.
9. Smith C, Chang MY, Parker KH, Beury DW, DuHadaway JB, Flick HE*, et al.* IDO is a nodal pathogenic driver of lung cancer and metastasis development. *Cancer Discov* **2012**;2(8):722-35.
10. Munn DH, Sharma MD, Baban B, Harding HP, Zhang Y, Ron D*, et al.* GCN2 kinase in T cells mediates proliferative arrest and anergy induction in response to indoleamine 2,3-dioxygenase. *Immunity* **2005**;22(5):633-42.
11. Sonner JK, Deumelandt K, Ott M, Thome CM, Rauschenbach KJ, Schulz S*, et al.* The stress kinase GCN2 does not mediate suppression of antitumor T cell responses by tryptophan catabolism in experimental melanomas. *Oncoimmunology* **2016**;5(12):e1240858.
12. Van de Velde LA, Guo XJ, Barbaric L, Smith AM, Oguin TH, 3rd, Thomas PG*, et al.* Stress Kinase GCN2 Controls the Proliferative Fitness and Trafficking of Cytotoxic T Cells Independent of Environmental Amino Acid Sensing. *Cell Rep* **2016**;17(9):2247-58.
13. Metz R, Rust S, Duhadaway JB, Mautino MR, Munn DH, Vahanian NN*, et al.* IDO inhibits a tryptophan sufficiency signal that stimulates mTOR: A novel IDO effector pathway targeted by D-1-methyl-tryptophan. *Oncoimmunology* **2012**;1(9):1460-8.
14. Fallarino F, Grohmann U, Vacca C, Bianchi R, Orabona C, Spreca A*, et al.* T cell apoptosis by tryptophan catabolism. *Cell Death Differ* **2002**;9:1069-77.
15. Terness P, Bauer TM, Rose L, Dufter C, Watzlik A, Simon H*, et al.* Inhibition of allogeneic T cell proliferation by indoleamine 2,3-dioxygenase-expressing dendritic cells: mediation of suppression by tryptophan metabolites. *J Exp Med* **2002**;196(4):447-57.
16. Fallarino F, Grohmann U, You S, McGrath BC, Cavener DR, Vacca C*, et al.* The combined effects of tryptophan starvation and tryptophan catabolites down-regulate T cell receptor zeta-chain and induce a regulatory phenotype in naive T cells. *J Immunol* **2006**;176(11):6752-61.
17. Mezrich JD, Fechner JH, Zhang X, Johnson BP, Burlingham WJ, Bradfield CA. An interaction between kynurenine and the aryl hydrocarbon receptor can generate regulatory T cells. *J Immunol* **2010**;185(6):3190-8.

18. Liu Y, Liang X, Dong W, Fang Y, Lv J, Zhang T*, et al.* Tumor-Repopulating Cells Induce PD-1 Expression in CD8(+) T Cells by Transferring Kynurenine and AhR Activation. *Cancer Cell* **2018**;33(3):480-94 e7.
19. Triplett TA, Garrison KC, Marshall N, Donkor M, Blazeck J, Lamb C*, et al.* Reversal of indoleamine 2,3-dioxygenase-mediated cancer immune suppression by systemic kynurenine depletion with a therapeutic enzyme. *Nature biotechnology* **2018**;36(8):758-64.
20. Munn DH, Zhou M, Attwood JT, Bondarev I, Conway SJ, Marshall B*, et al.* Prevention of allogeneic fetal rejection by tryptophan catabolism. *Science* **1998**;281:1191-3.
21. Uyttenhove C, Pilotte L, Theate I, Stroobant V, Colau D, Parmentier N*, et al.* Evidence for a tumoral immune resistance mechanism based on tryptophan degradation by indoleamine 2,3-dioxygenase. *Nat Med* **2003**;9(10):1269-74.
22. Hennequart M, Pilotte L, Cane S, Hoffmann D, Stroobant V, Plaen E*, et al.* Constitutive IDO1 Expression in Human Tumors Is Driven by Cyclooxygenase-2 and Mediates Intrinsic Immune Resistance. *Cancer Immunol Res* **2017**;5(8):695-709.
23. van Baren N, Van den Eynde BJ. Tryptophan-degrading enzymes in tumoral immune resistance. *Front Immunol* **2015**;6:34.
24. Spranger S, Spaapen RM, Zha Y, Williams J, Meng Y, Ha TT*, et al.* Up-regulation of PD-L1, IDO, and T(regs) in the melanoma tumor microenvironment is driven by CD8(+) T cells. *Sci Transl Med* **2013**;5(200):200ra116.
25. Godin-Ethier J, Hanafi LA, Piccirillo CA, Lapointe R. Indoleamine 2,3-dioxygenase expression in human cancers: clinical and immunologic perspectives. *Clin Cancer Res* **2011**;17(22):6985-91.
26. Koblish HK, Hansbury MJ, Bowman KJ, Yang G, Neilan CL, Haley PJ*, et al.* Hydroxyamidine inhibitors of indoleamine-2,3-dioxygenase potently suppress systemic tryptophan catabolism and the growth of IDO-expressing tumors. *Mol Cancer Ther* **2010**;9(2):489-98.
27. Holmgaard RB, Zamarin D, Munn DH, Wolchok JD, Allison JP. Indoleamine 2,3-dioxygenase is a critical resistance mechanism in antitumor T cell immunotherapy targeting CTLA-4. *J Exp Med* **2013**;210(7):1389-402.
28. Spranger S, Koblish HK, Horton B, Scherle PA, Newton R, Gajewski TF. Mechanism of tumor rejection with doublets of CTLA-4, PD-1/PD-L1, or IDO blockade involves restored IL-2 production and proliferation of CD8(+) T cells directly within the tumor microenvironment. *J Immunother Cancer* **2014**;2:3.
29. Yue EW, Sparks R, Polam P, Modi D, Douty B, Wayland B*, et al.* INCB24360 (Epacadostat), a Highly Potent and Selective Indoleamine-2,3-dioxygenase 1 (IDO1) Inhibitor for Immuno-oncology. *ACS Med Chem Lett* **2017**;8(5):486-91.
30. Amobi A, Qian F, Lugade AA, Odunsi K. Tryptophan Catabolism and Cancer Immunotherapy Targeting IDO Mediated Immune Suppression. *Adv Exp Med Biol* **2017**;1036:129-44.
31. Long GVD, R.; Hamid, O.; Gajewski, T.; Caglevic, C.: Dalle, S.; Arance, A.; Carlino, M. S.; Grob, J.-J.; Kim, T. M.; Demidov, L.; Robert, C.; Larkin, J.; Anderson, J. R.; Maleski, J.; Jones, M.; Diede, S. J.; Mitchell, T. C. . Epacadostat (E) plus pembrolizumab (P) versus pembrolizumab alone in patients (pts) with unresectable or metastatic melanoma: Results of the phase 3 ECHO-301/KEYNOTE-252 study. *J Clin Oncol* **2018**;36:(suppl; abstr 108).
32. Rose S. Companies Scaling Back IDO1 Inhibitor Trials. *Cancer Discov* **2018**;8(7):OF5.
33. Muller AJ, Manfredi MG, Zakharia Y, Prendergast GC. Inhibiting IDO pathways to treat cancer: lessons from the ECHO-301 trial and beyond. *Semin Immunopathol* **2018**.
34. Van den Eynde BJ, van Baren N, Baurain JF. Is there a clinical future for IDO1 inhibitors after the failure of epacadostat in melanoma? *Annu Rev Cancer Bio* **2019**;4(In press).
35. Badawy AA. Kynurenine Pathway of Tryptophan Metabolism: Regulatory and Functional Aspects. *Int J Tryptophan Res* **2017**;10:1178646917691938.
36. van Baren N, Van den Eynde BJ. Tumoral Immune Resistance Mediated by Enzymes That Degrade Tryptophan. *Cancer Immunol Res* **2015**;3(9):978-85.

37. Kanai M, Funakoshi H, Takahashi H, Hayakawa T, Mizuno S, Matsumoto K*, et al.* Tryptophan 2,3-dioxygenase is a key modulator of physiological neurogenesis and anxiety-related behavior in mice. *Mol Brain* **2009**;2(1):8.
38. Pilotte L, Larrieu P, Stroobant V, Colau D, Dolusic E, Frederick R*, et al.* Reversal of tumoral immune resistance by inhibition of tryptophan 2,3-dioxygenase. *Proc Natl Acad Sci USA* **2012**;109(7):2497-502.
39. Opitz CA, Litzenburger UM, Sahm F, Ott M, Tritschler I, Trump S*, et al.* An endogenous tumour-promoting ligand of the human aryl hydrocarbon receptor. *Nature* **2011**;478(7368):197-203.
40. Hoffmann D, Dvorakova T, Stroobant V, Solvay M, Klaessens S, Letellier M-C*, et al.* Tryptophan 2,3-dioxygenase expression is prominent in human hepatocarcinoma cells, but is mostly restricted to pericytes in other human tumors. *Cancer Immunol Res* **2019**;co-submitted.
41. Dolusic E, Larrieu P, Moineaux L, Stroobant V, Pilotte L, Colau D*, et al.* Tryptophan 2,3-Dioxygenase (TDO) Inhibitors. 3-(2-(Pyridyl)ethenyl)indoles as Potential Anticancer Immunomodulators. *J Med Chem* **2011**;54(15):5320-34.
42. Meininger D, Zalameda L, Liu Y, Stepan LP, Borges L, McCarter JD*, et al.* Purification and kinetic characterization of human indoleamine 2,3-dioxygenases 1 and 2 (IDO1 and IDO2) and discovery of selective IDO1 inhibitors. *Biochimica et biophysica acta* **2011**;1814(12):1947-54.
43. Metz R, Duhadaway JB, Kamasani U, Laury-Kleintop L, Muller AJ, Prendergast GC. Novel tryptophan catabolic enzyme IDO2 is the preferred biochemical target of the antitumor indoleamine 2,3-dioxygenase inhibitory compound D-1-methyl-tryptophan. *Cancer Res* **2007**;67(15):7082-7.
44. Maeta A, Fukuwatari T, Funakoshi H, Nakamura T, Shibata K. Tryptophan-restriction diets help to maintain L-tryptophan homeostasis in tryptophan 2,3-dioxygenase knockout mice. *Int J Tryptophan Res* **2013**;6(Suppl 1):55-65.
45. Crosignani S, Cauwenberghs S, Driessens G, Deroose F. Novel 3-(indol-3yl)-pyridine derivatives, pharmaceutical composition and methods for use. U.S. Patent Application 20150225367-A1, filed February 11th, 2015.
46. Liu X, Shin N, Koblish HK, Yang G, Wang Q, Wang K*, et al.* Selective inhibition of IDO1 effectively regulates mediators of antitumor immunity. *Blood* **2010**;115(17):3520-30.
47. Wiig H, Aukland K, Tenstad O. Isolation of interstitial fluid from rat mammary tumors by a centrifugation method. *Am J Physiol Heart Circ Physiol* **2003**;284(1):H416-24.
48. Pantouris G, Serys M, Yuasa HJ, Ball HJ, Mowat CG. Human indoleamine 2,3-dioxygenase-2 has substrate specificity and inhibition characteristics distinct from those of indoleamine 2,3-dioxygenase-1. *Amino acids* **2014**;46(9):2155-63.
49. Zhu J, Powis de Tenbossche CG, Cane S, Colau D, van Baren N, Schmitt-Verhulst AM*, et al.* Resistance to cancer immunotherapy mediated by apoptosis of tumor-infiltrating lymphocytes. *Nat Commun* **2017**;8(1):1404.
50. Huijbers IJ, Krimpenfort P, Chomez P, van der Valk MA, Song JY, Inderberg-Suso EM*, et al.* An inducible mouse model of melanoma expressing a defined tumor antigen. *Cancer Res* **2006**;66(6):3278-86.
51. Lanz TV, Williams SK, Stojic A, Iwantscheff S, Sonner JK, Grabitz C*, et al.* Tryptophan-2,3-Dioxygenase (TDO) deficiency is associated with subclinical neuroprotection in a mouse model of multiple sclerosis. *Sci Rep* **2017**;7:41271.
52. Ferreira P, Shin I, Sosova I, Dornevil K, Jain S, Dewey D*, et al.* Hypertryptophanemia due to tryptophan 2,3-dioxygenase deficiency. *Mol Genet Metab* **2017**;120(4):317-24.
53. Munn DH, Shafizadeh E, Attwood JT, Bondarev I, Pashine A, Mellor AL. Inhibition of T cell proliferation by macrophage tryptophan catabolism. *J Exp Med* **1999**;189:1363-72.
54. Kudo Y, Boyd CA. Characterisation of L-tryptophan transporters in human placenta: a comparison of brush border and basal membrane vesicles. *J Physiol* **2001**;531(Pt 2):405-16.

55. Qian F, Villella J, Wallace PK, Mhawech-Fauceglia P, Tario JD, Jr., Andrews C*, et al.* Efficacy of levo-1-methyl tryptophan and dextro-1-methyl tryptophan in reversing indoleamine-2,3-dioxygenase-mediated arrest of T-cell proliferation in human epithelial ovarian cancer. *Cancer Res* **2009**;69(13):5498-504.
56. Saha A, Chatterjee SK. Combination of CTL-associated antigen-4 blockade and depletion of CD25 regulatory T cells enhance tumour immunity of dendritic cell-based vaccine in a mouse model of colon cancer. *Scand J Immunol* **2010**;71(2):70-82.
57. Woo SR, Turnis ME, Goldberg MV, Bankoti J, Selby M, Nirschl CJ*, et al.* Immune inhibitory molecules LAG-3 and PD-1 synergistically regulate T-cell function to promote tumoral immune escape. *Cancer Res* **2012**;72(4):917-27.
58. Zippelius A, Schreiner J, Herzig P, Muller P. Induced PD-L1 expression mediates acquired resistance to agonistic anti-CD40 treatment. *Cancer Immunol Res* **2015**;3(3):236-44.
59. Badiola I, Olaso E, Crende O, Friedman SL, Vidal-Vanaclocha F. Discoidin domain receptor 2 deficiency predisposes hepatic tissue to colon carcinoma metastasis. *Gut* **2012**;61(10):1465-72.
60. Arabzadeh A, Chan C, Nouvion AL, Breton V, Benlolo S, DeMarte L*, et al.* Host-related carcinoembryonic antigen cell adhesion molecule 1 promotes metastasis of colorectal cancer. *Oncogene* **2013**;32(7):849-60.
61. Ochoa MC, Fioravanti J, Duitman EH, Medina-Echeverz J, Palazon A, Arina A*, et al.* Liver gene transfer of interkeukin-15 constructs that become part of circulating high density lipoproteins for immunotherapy. *PLoS One* **2012**;7(12):e52370.
62. Salter M, Hazelwood R, Pogson CI, Iyer R, Madge DJ. The effects of a novel and selective inhibitor of tryptophan 2,3-dioxygenase on tryptophan and serotonin metabolism in the rat. *Biochem Pharmacol* **1995**;49:1435-42.
63. Röhrig UF, Zoete V, Michielin O. Inhibitors of the Kynurenine Pathway. *In: Waring MJ (eds) Cancer II Topics in Medicinal Chemistry* **2017**;28.
64. Prendergast GC, Mondal A, Dey S, Laury-Kleintop LD, Muller AJ. Inflammatory Reprogramming with IDO1 Inhibitors: Turning Immunologically Unresponsive 'Cold' Tumors 'Hot'. *Trends Cancer* **2018**;4(1):38-58.
65. Mondal A, Smith C, DuHadaway JB, Sutanto-Ward E, Prendergast GC, Bravo-Nuevo A*, et al.* IDO1 is an Integral Mediator of Inflammatory Neovascularization. *EBioMedicine* **2016**;14:74-82.
66. Muller AJ, Sharma MD, Chandler PR, Duhadaway JB, Everhart ME, Johnson BA, 3rd*, et al.* Chronic inflammation that facilitates tumor progression creates local immune suppression by inducing indoleamine 2,3 dioxygenase. *Proc Natl Acad Sci USA* **2008**;105(44):17073-8.
67. Muller AJ, DuHadaway JB, Donover PS, Sutanto-Ward E, Prendergast GC. Inhibition of indoleamine 2,3-dioxygenase, an immunoregulatory target of the cancer suppression gene Bin1, potentiates cancer chemotherapy. *Nat Med* **2005**;11(3):312-9.
68. Li M, Bolduc AR, Hoda MN, Gamble DN, Dolisca SB, Bolduc AK*, et al.* The indoleamine 2,3-dioxygenase pathway controls complement-dependent enhancement of chemo-radiation therapy against murine glioblastoma. *J Immunother Cancer* **2014**;2:21.
69. Gao J, Deng F, Jia W. Inhibition of Indoleamine 2,3-Dioxygenase Enhances the Therapeutic Efficacy of Immunogenic Chemotherapeutics in Breast Cancer. *J Breast Cancer* **2019**;22(2):196-209.
70. Johnson TS, McGaha T, Munn DH. Chemo-Immunotherapy: Role of Indoleamine 2,3-Dioxygenase in Defining Immunogenic Versus Tolerogenic Cell Death in the Tumor Microenvironment. *Adv Exp Med Biol* **2017**;1036:91-104.
71. Hou DY, Muller AJ, Sharma MD, DuHadaway J, Banerjee T, Johnson M*, et al.* Inhibition of indoleamine 2,3-dioxygenase in dendritic cells by stereoisomers of 1-methyl-tryptophan correlates with antitumor responses. *Cancer Res* **2007**;67(2):792-801.

72. Hsu YL, Hung JY, Chiang SY, Jian SF, Wu CY, Lin YS*, et al.* Lung cancer-derived galectin-1 contributes to cancer associated fibroblast-mediated cancer progression and immune suppression through TDO2/kynurenine axis. *Oncotarget* **2016**;7(19):27584-98.
73. Bhutia YD, Babu E, Ramachandran S, Ganapathy V. Amino Acid transporters in cancer and their relevance to "glutamine addiction": novel targets for the design of a new class of anticancer drugs. *Cancer Res* **2015**;75(9):1782-8.
74. Timosenko E, Ghadbane H, Silk JD, Shepherd D, Gileadi U, Howson LJ*, et al.* Nutritional Stress Induced by Tryptophan-Degrading Enzymes Results in ATF4-Dependent Reprogramming of the Amino Acid Transporter Profile in Tumor Cells. *Cancer Res* **2016**;76(21):6193-204.
75. Tina E, Prosen S, Lennholm S, Gasparyan G, Lindberg M, Gothlin Eremo A. Expression profile of the amino acid transporters SLC7A5, SLC7A7, SLC7A8 and the enzyme TDO2 in basal cell carcinoma. *Br J Dermatol* **2018**.
76. Hvid H, Fendt SM, Blouin MJ, Birman E, Voisin G, Svendsen AM*, et al.* Stimulation of MC38 tumor growth by insulin analog X10 involves the serine synthesis pathway. *Endocr Relat Cancer* **2012**;19(4):557-74.
77. Pigatto MC, Mossmann DL, Dalla Costa T. HPLC-UV method for quantifying etoposide in plasma and tumor interstitial fluid by microdialysis: application to pharmacokinetic studies. *Biomed Chromatogr* **2015**;29(4):529-36.
78. Ait-Belkacem R, Bol V, Hamm G, Schramme F, Van Den Eynde B, Poncelet L*, et al.* Microenvironment Tumor Metabolic Interactions Highlighted by qMSI: Application to the Tryptophan-Kynurenine Pathway in Immuno-Oncology. *SLAS Discov* **2017**;22(10):1182-92.

Table 1. Structure, in vitro activity and in vivo pharmacokinetic profile of TDO inhibitor PF06845102/EOS200809

Structure of PF06845102/EOS200809		
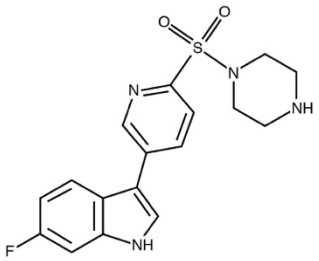		
Enzymatic activity assay[1]		
Cell line	**IC_{50} (nM)**	
A172 human cells		
hTDO	230 +/- 49	(n=9)
293-E transfected human cells		
hTDO	285 +/- 22	(n=10)
hIDO1	>10000	(n=2)
hIDO2 (full length)	NE	(n=2)
P815B transfected mouse cells		
hTDO	211 +/- 24	(n=8)
mIDO1	>10000	(n=2)
mTDO	104 +/- 16	(n=12)
hIDO2 (full length)	NE	(n=2)
hIDO2 (short length)	NE	(n=2)
CT26 transfected mouse cells		
mTDO	205 +/- 70	(n=4)
Mouse pharmacokinetics[2]		
Clearance	30 mL/h/kg	
$T_{1/2}$ after IV administration	2.5 h	
$T_{1/2}$ after oral administration	4.2 h	
Oral bioavailability (100 mg/kg)	80 %	
AUC after oral administration (100 mg/kg)	45000 h*ng/mL	

[1]Cellular assays based on TDO or IDO-expressing human A172 and 293-E cells as well as murine P815B and CT26 cells were used to measure IC_{50}, defined as the concentration giving 50% inhibition of kynurenine production at a L-tryptophan concentration of 80µM. Results are expressed as mean ± SD. N represents the number of independent experiments. NE = not evaluable due to undetectable hIDO2 activity, even under conditions of increased Trp concentration (3mM) and prolonged incubation time (24 and 48 hours).

[2]PK was measured on 3 mice IV and 3 mice for oral administration. AUC: area under the curve.

Legends

Figure 1. TDO inhibitor PF06845102/EOS200809 prevents *in vivo* degradation of tryptophan into kynurenine

Effect of TDOi was assessed *in vivo* in naive mice. Trp and Kyn concentrations were measured by LC-MS/MS (**A**) in whole liver extract or (**B**) in plasma of BALB/c mice 2h, 8h and 16h after treatment with different concentrations of PF06845102/EOS200809 (TDOi). Histograms represent an average of n=6 to 8 mice. (**C**) Basal level of Trp and Kyn were also measured in tumor interstitial fluid (ISF) of CT26 or CT26mTDO tumors from mice treated with the vehicle or PF06845102/EOS200809 (100mg/kg) 2h before the tumor samplings. Each symbol represents an individual mouse. Error bars represent the mean ± SEM. The experiment is representative of at least 2 independent experiments. Mann-Whitney unpaired T-test with Bonferroni correction factor (*p<0.05, **p<0.01,***p<0.001,****p<0.0001).

Figure 2. Synergistic anti-tumor effect of anti-CTLA4 and TDO inhibitor

BALB/c mice were implanted subcutaneously with 10^5 CT26mTDO (**A**) or vector-control CT26ev (**B**) tumor cells. Nine days post-challenge, they were randomized and treated with 3 injections (60 µg) of anti-CTLA4 on day 9/12/15, with the TDO inhibitor PF06845102/EOS200809 (TDOi) orally twice a day (100mg/kg), or with the combined anti-CTLA4 and TDO inhibitor therapy. The graphs on the left show the % tumor-free mice and the small graphs on the right represent the individual tumor growth curves for each mouse. The fractions on graphs indicate the number of tumor-free mice at day 100. The experiment (10 mice per group) is representative of 3 independent experiments. Statistical significance of differences in % tumor- free mice was calculated using a log-rank (Mantel-Cox) test. (**C**) Individual CT26mTDO growth curves of all mice from 3 independent experiments are plotted after fitting a mixed linear model to normalize tumor growth and treatment effect. The normalized tumor growth represents the growth of the tumor for each mouse at a specific time

compared to the average growth of all the tumors in this experiment at that time. Growth curves above the reference line are higher than the average of the corresponding experiment, growth curves below the reference line are lower than the average of the corresponding experiment. Treatment effect was compared using a F-statistic (p=0.0004).

Figure 3. Tryptophan and kynurenine levels in the blood of WT, TDO-KO, IDO1-KO and double IDO1/TDO-KO mice

Tryptophan (**A**) and kynurenine (**B**) concentrations (µM) were determined by HPLC-UV in the serum of wild type (WT) B/6, TDO-KO, IDO1-KO or double IDO1/TDO-KO B/6 mice (20 to 26 mice per genotype). Each single symbol represents an individual mouse. Error bars show the mean ± SEM. Data shown come from 2 pooled independent experiments. Mann-Whitney unpaired T-test with Bonferroni correction factor (****p<0.0001).

Figure 4. Increased efficacy of checkpoint inhibitors in TDO-KO mice

TDO-KO or WT littermate mice were challenged subcutaneously with 5.10^5 MC38 tumor cells. Mice were randomized after 8-10 days and received 4 i.p. injections every 3 days of (**A**) anti-CTLA4 (30/30/3/60 µg; day 10/13/16/20) or (**B**) anti-PD1 (100/100/200/200 µg; day 8/11/14/17).. Graphs represent tumor volume mean ± SEM. The experiment is representative of 3 independent experiments. Two-way ANOVA (*p<0.05, ***p<0.001).

(**C**) MC38 tumors were established in TDO-KO and WT littermates as above and treated with anti-PD1 or control IgG2a (200/100/10 µg; day 7/10/13). Tumors were collected on days 6, 9, 13 and 15 (5 mice per time point) and analyzed by RT-qPCR for the presence of CD8β mRNA. Each symbol represents an individual mouse (n=20 and n=14 for IgG2a and anti-PD1 treated groups respectively). Bars show the median. Data from one experiment representative of two. Mann-Whitney unpaired T-test (*p<0.5, **p<0.01). The same tumors from anti-PD1- treated TDO-KO and WT mice sacrificed between days 13 and 15 were evaluated by immunohistochemistry for the presence of (**D**) $CD8^+$, (**E**) $CD4^+$ and (**F**) $CD3^+$ cells in the indicated tumor regions. Tumor sections were stained with rabbit monoclonal anti-CD8, anti-

CD4 or anti-CD3 antibody. Histological images were obtained using a digital slide scanner. For each staining, the percentage of positive cells was measured using the Halo™ Image Analysis software. Each symbol represents the tumor section of an individual mouse (n=8 to 9 for each group). Error bars show the mean ± SEM. Mann-Whitney unpaired T-test (**p<0.001).

Figure 5. Loss of anti-PD1 efficacy in TDO-KO mice fed with Trp-low diet

Two days before subcutaneous MC38 challenge (5.10^5 cells), TDO-KO (**A**) or WT (**B**) littermate mice started being fed with a standard diet (0.18% Trp) or a Trp-low diet (0.06% Trp) for the duration of the experiment. At day 7 post-challenge, they were randomized and treated with anti-PD1 or IgG2a i.p. (100 µg every 3 days).. Graphs represent tumor volume mean ± SEM. Data from one experiment representative of two. Two-way ANOVA (**p<0.001). Trp and Kyn concentrations in the (**C**) serum, (**D**) tumor homogenate and (**E**) tumor interstitial fluid were measured by HPLC-UV in samples from tumor-bearing mice fed with standard or Trp-low diet, which were collected 34 days after subcutaneous injection of MC38 cells. A fragment of each tumor was immediately homogenized in PBS with Ultra-Turrax. Another fragment was centrifuged at 420 g on a 20µM filter to collect the interstitial fluid. Each symbol represents an individual mouse. N=10 mice per group, except for the interstitial fluid (standard diet TDO-KO: n=8; standard diet WT: n=6; Trp-low diet TDO-KO: n=9; Trp-low diet WT: n=7). Error bars show the mean ± SEM. The experiment is representative of 2 independent experiments. Mann-Whitney unpaired T-test (**p<0.001, ***p<0.001, ****p<0.0001)

Figure 6. IDO1-mediated immunosuppression is overruled in TDO-KO mice

(**A**) MC38 tumors obtained in Figure 5C were tested by RT-qPCR for the expression of IDO1, IFNγ and TDO2. Bars show the median. Data from one experiment representative of two. Mann-Whitney unpaired T-test (*p<0.05, **p<0.001). (**B**) Littermate WT and (**C**) TDO-KO mice were implanted subcutaneously with 5.10^5 MC38 tumor cells. The next day, mice started being treated with epacadostat or vehicle by oral gavage twice a day (100mg/kg). From day 7, they received 3 injections of 100 µg anti-PD1 or IgG2a control every 3 days. Graphs represent

923 tumor volume mean ± SEM. Data from one experiment representative of two. Two-way
924 ANOVA (***p<0.001, ****p<0.0001).
925
926

Figure 1

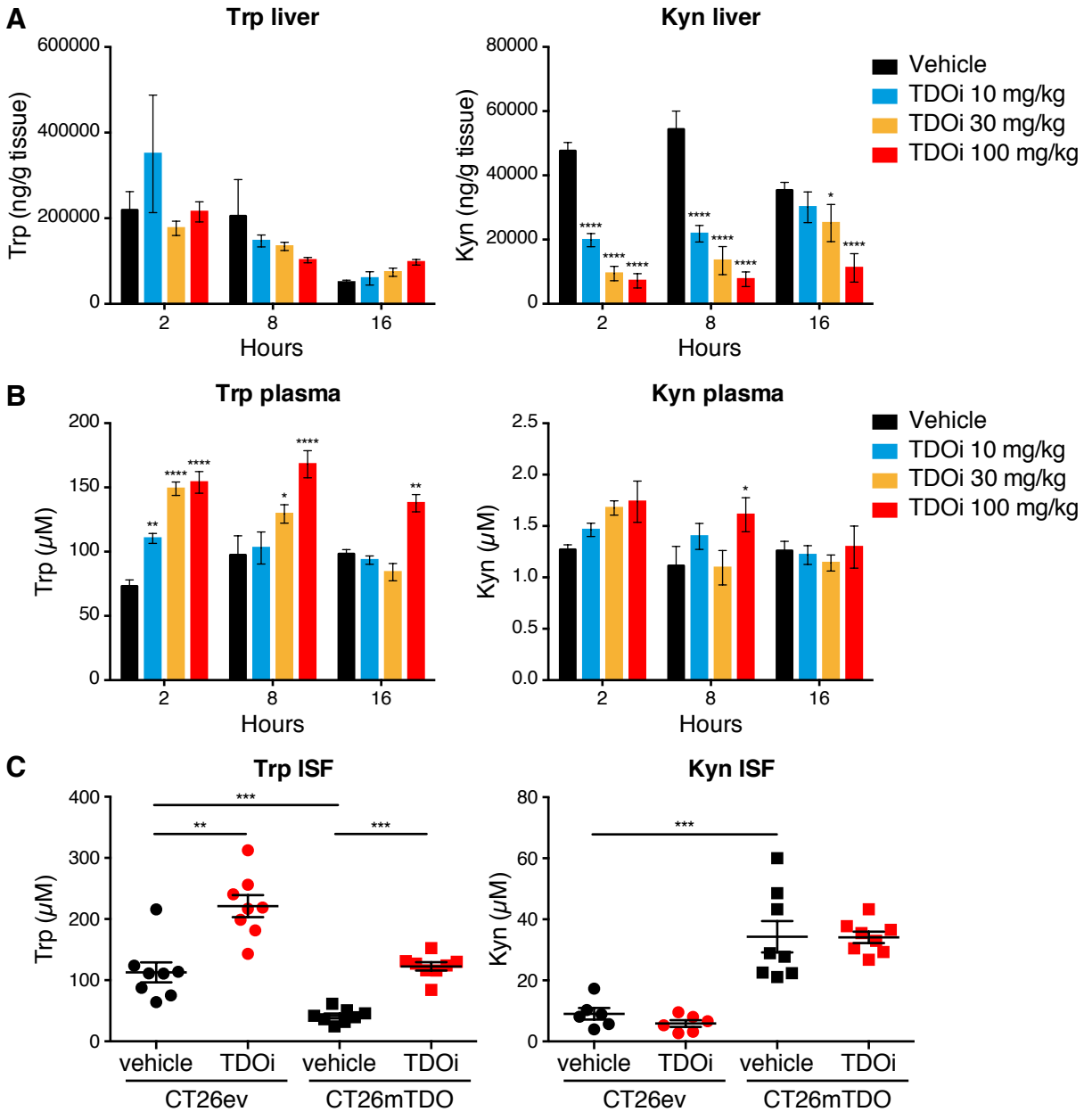
A
Trp liver
Trp (ng/g tissue)
600000
400000
200000
0
2
8
16
Hours
Kyn liver
Kyn (ng/g tissue)
80000
60000
40000
20000
0
Vehicle
TDOi 10 mg/kg
TDOi 30 mg/kg
TDOi 100 mg/kg
B
Trp plasma
Trp (μM)
200
150
100
50
0
Kyn plasma
Kyn (μM)
2.5
2.0
1.5
1.0
0.5
0.0
C
Trp ISF
Trp (μM)
400
300
200
100
0
vehicle
TDOi
CT26ev
CT26mTDO
Kyn ISF
Kyn (μM)
80
60
40
20

Figure 2

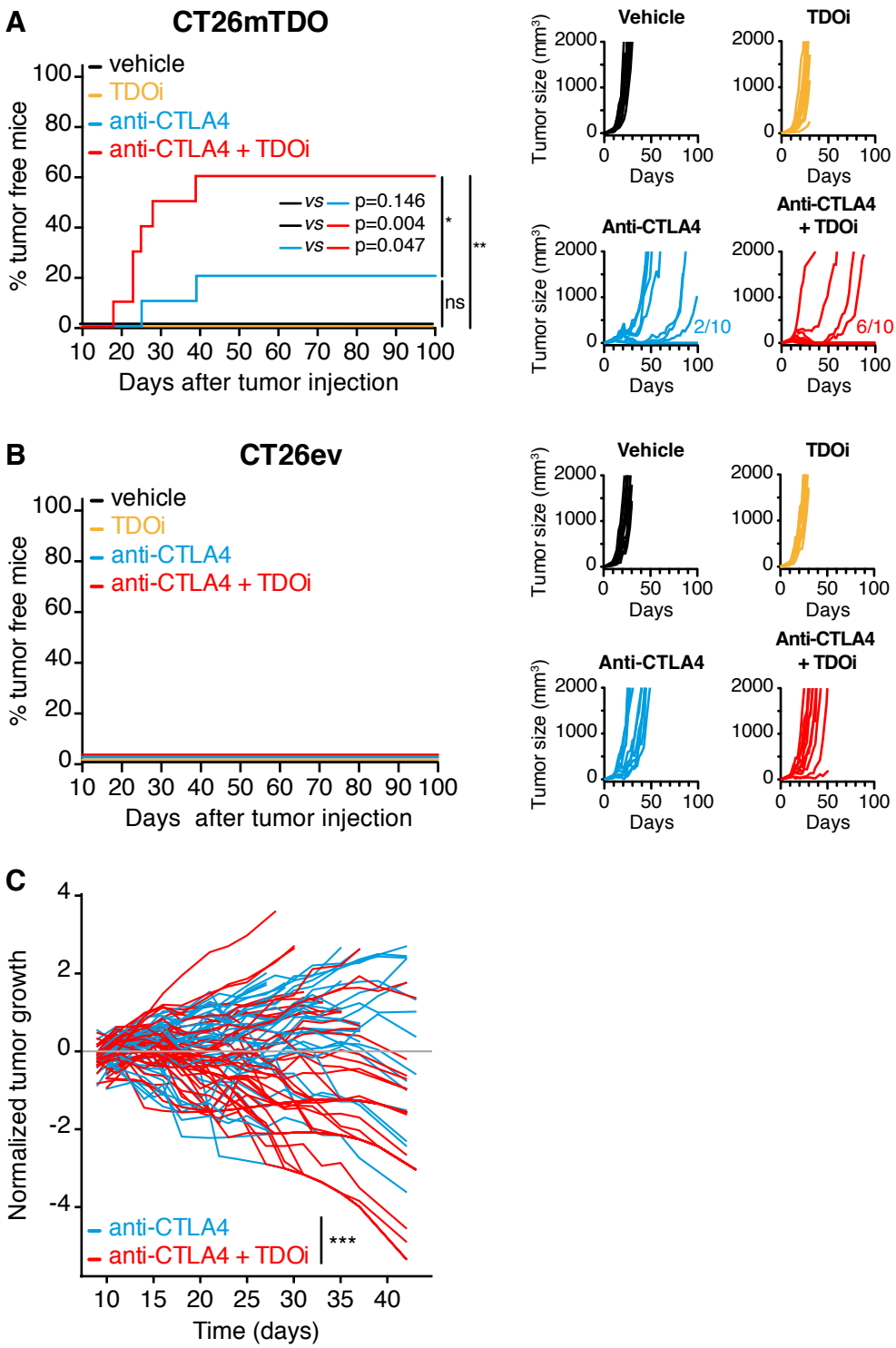
A
CT26mTDO
vehicle
TDOi
anti-CTLA4
anti-CTLA4 + TDOi
% tumor free mice
vs p=0.146
vs p=0.004
vs p=0.047
*
**
ns
Days after tumor injection
Vehicle
TDOi
Anti-CTLA4
Anti-CTLA4 + TDOi
Tumor size (mm3)
Days
2/10
6/10
B
CT26ev
C
Normalized tumor growth
anti-CTLA4
anti-CTLA4 + TDOi
***
Time (days)

Figure 3

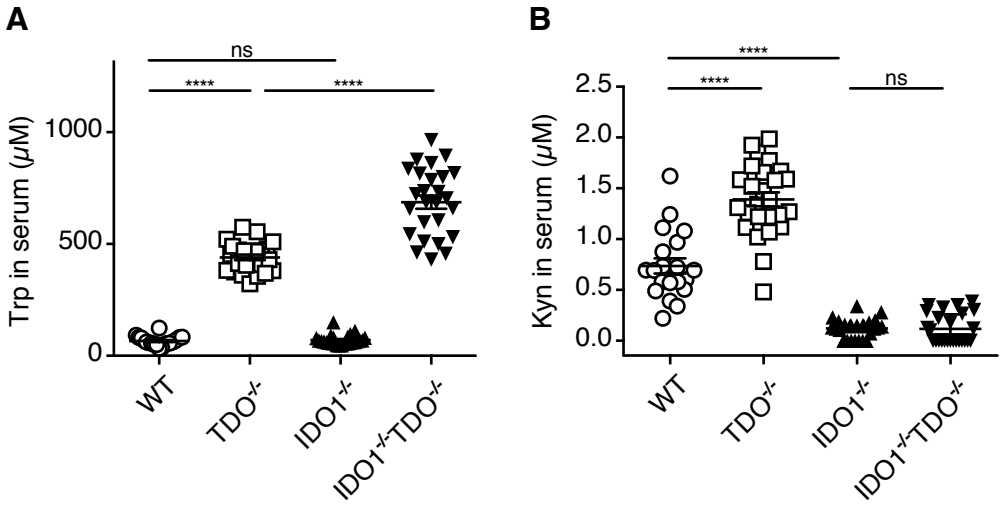
A
B
ns
****
****
****
****
ns
Trp in serum (μM)
Kyn in serum (μM)
1000
500
0
2.5
2.0
1.5
1.0
0.5
0.0
WT
TDO-/-
IDO1-/-
IDO1-/-TDO-/-

Figure 4

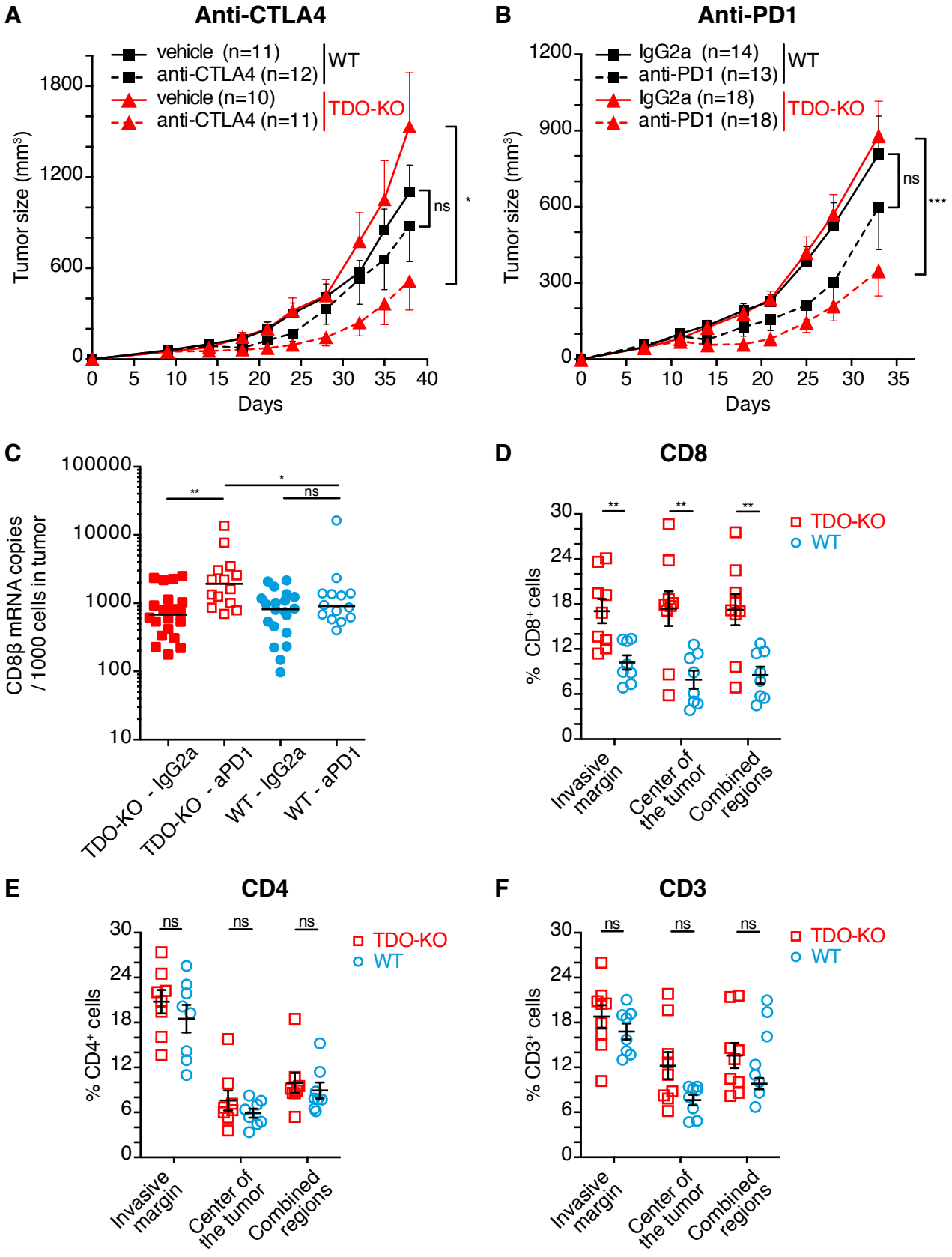
A
Anti-CTLA4
vehicle (n=11)
anti-CTLA4 (n=12)
vehicle (n=10)
anti-CTLA4 (n=11)
WT
TDO-KO
Tumor size (mm³)
Days
ns
*
B
Anti-PD1
IgG2a (n=14)
anti-PD1 (n=13)
IgG2a (n=18)
anti-PD1 (n=18)
WT
TDO-KO
Tumor size (mm³)
Days
ns
***
C
CD8β mRNA copies / 1000 cells in tumor
**
*
ns
TDO-KO - IgG2a
TDO-KO - aPD1
WT - IgG2a
WT - aPD1
D
CD8
% CD8⁺ cells
**
TDO-KO
WT
Invasive margin
Center of the tumor
Combined regions
E
CD4
% CD4⁺ cells
ns
TDO-KO
WT
Invasive margin
Center of the tumor
Combined regions
F
CD3
% CD3⁺ cells
ns
TDO-KO
WT
Invasive margin
Center of the tumor
Combined regions

Figure 5

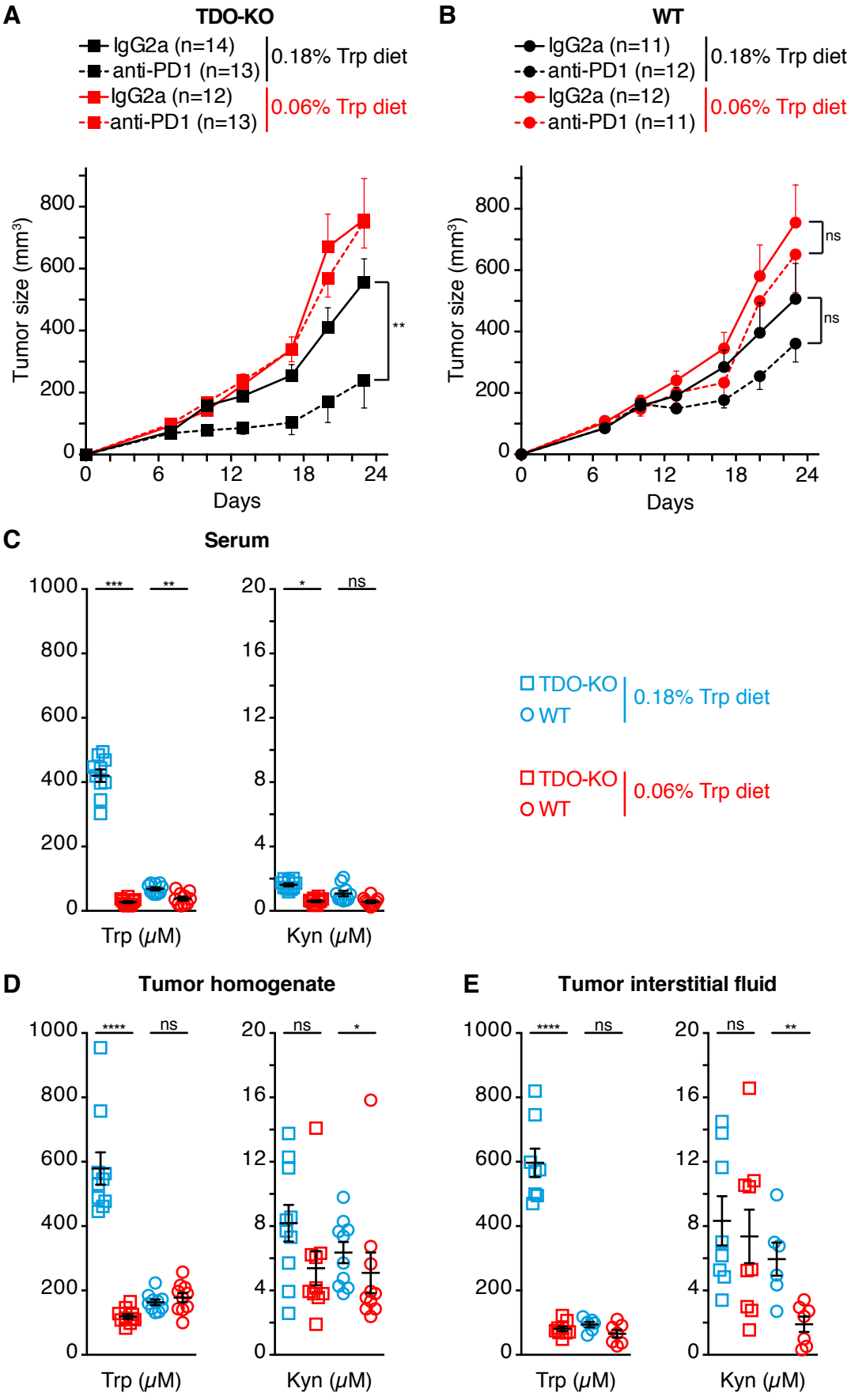
A
TDO-KO
IgG2a (n=14)
anti-PD1 (n=13)
0.18% Trp diet
IgG2a (n=12)
anti-PD1 (n=13)
0.06% Trp diet
Tumor size (mm³)
Days
**
B
WT
IgG2a (n=11)
anti-PD1 (n=12)
0.18% Trp diet
IgG2a (n=12)
anti-PD1 (n=11)
0.06% Trp diet
ns
ns
C
Serum
***
**
*
ns
Trp (μM)
Kyn (μM)
TDO-KO
WT
0.18% Trp diet
TDO-KO
WT
0.06% Trp diet
D
Tumor homogenate
****
ns
ns
*
E
Tumor interstitial fluid
****
ns
ns
**

Figure 6

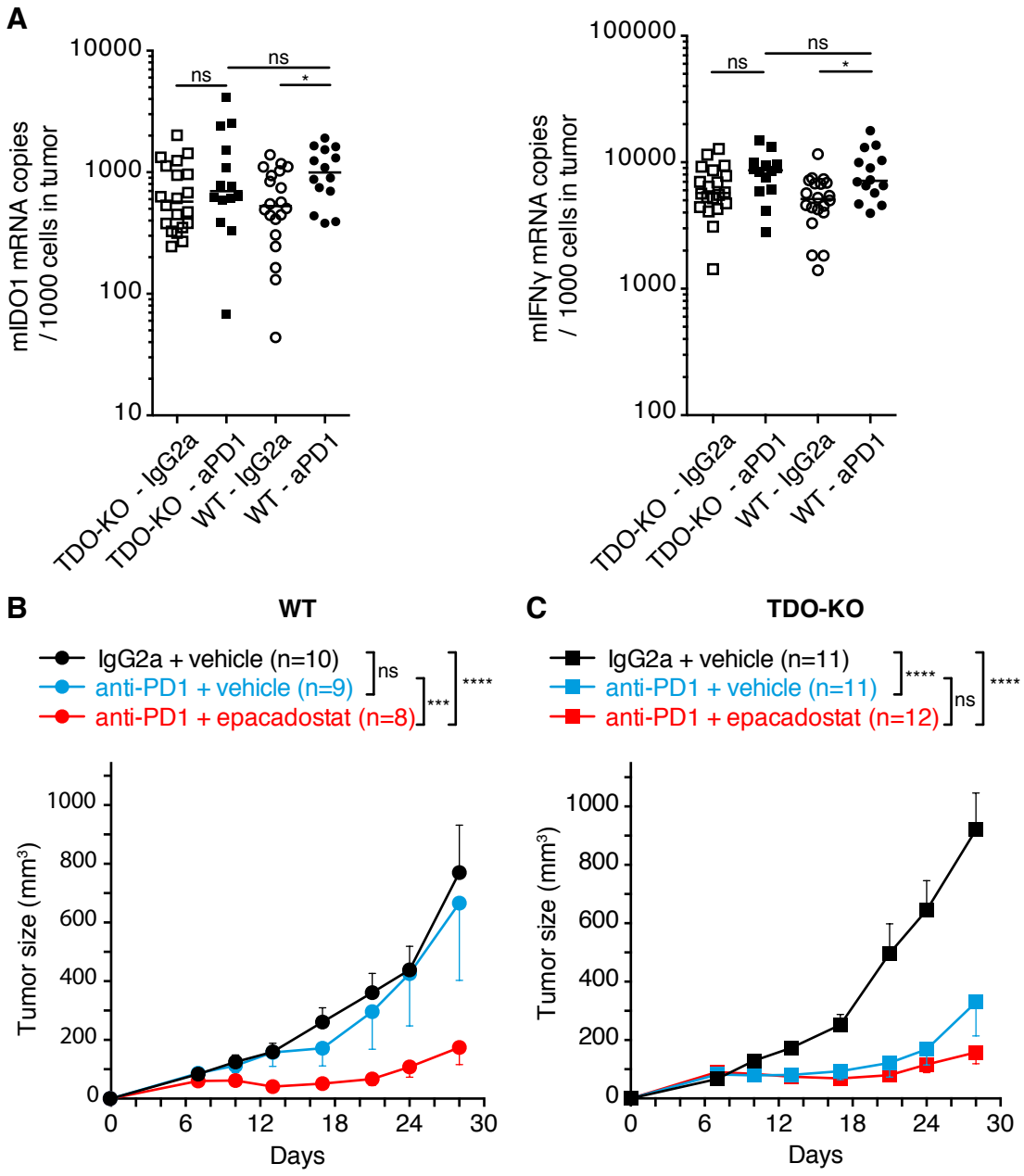
A
mIDO1 mRNA copies / 1000 cells in tumor
10000
1000
100
10
ns
ns
*
TDO-KO - IgG2a
TDO-KO - aPD1
WT - IgG2a
WT - aPD1
mIFNγ mRNA copies / 1000 cells in tumor
100000
10000
1000
100
ns
ns
*
TDO-KO - IgG2a
TDO-KO - aPD1
WT - IgG2a
WT - aPD1
B
WT
IgG2a + vehicle (n=10)
anti-PD1 + vehicle (n=9)
anti-PD1 + epacadostat (n=8)
ns
***
****
Tumor size (mm³)
1000
800
600
400
200
0
0
6
12
18
24
30
Days
C
TDO-KO
IgG2a + vehicle (n=11)
anti-PD1 + vehicle (n=11)
anti-PD1 + epacadostat (n=12)
****
ns
****
Tumor size (mm³)
1000
800
600
400
200
0
0
6
12
18
24
30
Days